Bioorganic & Medicinal Chemistry 22 (2014) 2253–2260

Contents lists available at ScienceDirect

Bioorganic & Medicinal Chemistry

journal homepage: www.elsevier.com/locate/bmc

Using 'biased-privileged' scaffolds to identify lysine methyltransferase inhibitors

Sudhir Kashyap [a,b,*], Joel Sandler [a], Ulf Peters [a], Eduardo J. Martinez [a], Tarun M. Kapoor [a,*]

[a] Laboratory of Chemistry and Cell Biology, Rockefeller University, New York, NY 10065, USA
[b] Organic & Biomolecular Chemistry Division, CSIR-Indian Institute of Chemical Technology, Hyderabad 500007, AP, India

ARTICLE INFO

Article history:
Received 14 December 2013
Revised 10 February 2014
Accepted 10 February 2014
Available online 28 February 2014

Keywords:
Post-translational modifications
KMTases
SET7
'Privileged' scaffolds
Inhibitors

ABSTRACT

Methylation of histones by lysine methyltransferases (KMTases) plays important roles in regulating chromatin function. It is also now clear that improper KMTases activity is linked to human diseases, such as cancer. We report an approach that employs drug-like 'privileged' scaffolds biased with motifs present in *S*-adenosyl methionine, the cofactor used by KMTases, to efficiently generate inhibitors for Set7, a biochemically well-characterized KMTase. Setin-1, the most potent inhibitor of Set7 we have developed also inhibits the KMTase G9a. Together these data suggest that these inhibitors should provide good starting points to generate useful probes for KMTase biology and guide the design of KMTase inhibitors with drug-like properties.

1. Introduction

Covalent and reversible post-translational modifications (PTMs) of histones, proteins that assemble into octamers around which DNA is 'spooled', play key roles in regulating gene expression in eukaryotes.[1–3] The histone-based structures, called nucleosomes, are the basic building blocks of chromatin.[4] In current models, PTMs of histone, such as acetylation, methylation, phosphorylation, glycosylation, sumoylation or ubiquitination, modulate protein recruitment to nucleosomes and can regulate chromatin organization.[5–8] For example, methylation of lysine-4 at the N-terminus of histone H3 recruits different proteins to chromatin and is believed to 'mark' a transcriptionally active 'on'-state of chromatin.[9,10] Like other dynamic PTMs, the level of histone lysine methylation is regulated by a balance in the activity of lysine methyltransferases (KMTases), which add the methyl group, and demethylases, which reverse the modification.[11] While important advances have been made in identifying KMTases, our understanding of the dynamic regulation and function of the different histone methylations remains incomplete. In line with critical roles of these enzymes in basic cellular processes, their dysfunction has been linked to human diseases, such as cancer.[12] Therefore, developing small molecule inhibitors of KMTases to probe their functions and to properly validate these enzymes as targets for chemotherapy has become an important goal.

It has been estimated that there are over 50 lysine methyltransferases in humans.[13,14] Currently, selective inhibitors for a handful of KMTases (e.g., G9a and Dot1L) have been reported.[15–17] However, when compared to other important enzyme targets (e.g., kinases),[18] the chemical diversity of available KMTase inhibitors and structural information on the modes of inhibition is restricted to a few examples. Therefore, designing probes for different KMTases remains challenging.

KMTases use *S*-adenosyl methionine (SAM) as the source of the methyl group in the reaction they catalyze (Fig. 1A). Structural analyses of KMTases have provided insight into how these enzymes bind this cofactor.[19,20] Unlike kinases, in which the ATP's phosphate groups are polar and the key hydrophobic contacts are made with the adenine, KMTases make numerous contacts with most of the atoms in SAM. Consistent with these observations SAM-related compounds, such as sinefungin and *S*-adenosylhomocysteine, inhibit KMTases and have been useful in studies analyzing their activities (Fig. 1B).[21–25] In addition, systematic modifications of SAM have led to the development of inhibitors of KMTases.[16,17] Encouraged by these findings, we developed a strategy that uses features of SAM to develop drug-like inhibitors for KMTases. We reasoned that 'privileged' chemical scaffolds, which have provided good starting points for developing inhibitors for different enzymes (e.g., kinases and myosins),[26,27] may be

* Corresponding authors. Tel.: +91 402 716 1649; fax: +91 402 716 0387 (S.K.); tel.: +1 212 327 8173; fax: +1 212 327 7358 (T.M.K.).
E-mail addresses: skashyap@iict.res.in (S. Kashyap), kapoor@rockefeller.edu (T.M. Kapoor).

http://dx.doi.org/10.1016/j.bmc.2014.02.024
0968-0896/

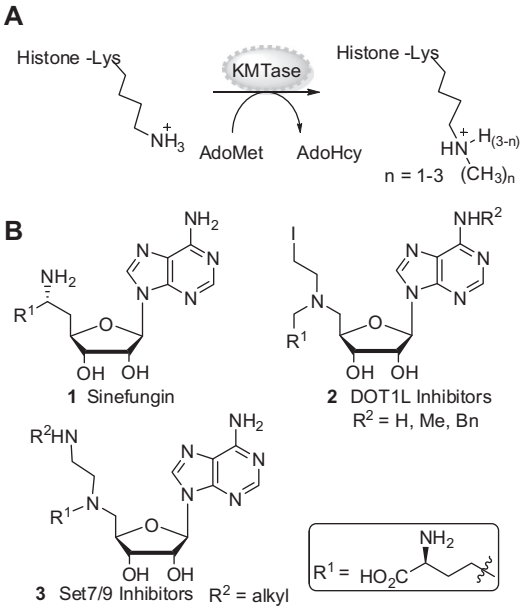

Figure 1. (A) Schematic for the KMTase catalyzed reaction. (B) SAM-based inhibitors of KMTases.

coupled to homocysteine to yield broad specificity KMTase inhibitors (Fig. 2A). In particular, the heterocycles (e.g., diaminopyrimidine and indoles) common in many kinase inhibitors could mimic the adenosine and a benzyl linkage to the homocysteine could position the key functional groups in correct spacing and orientations. Here we report the design, development and validation of SETin-1, an inhibitor of histone KMTases based on 'biased-privileged' scaffolds.

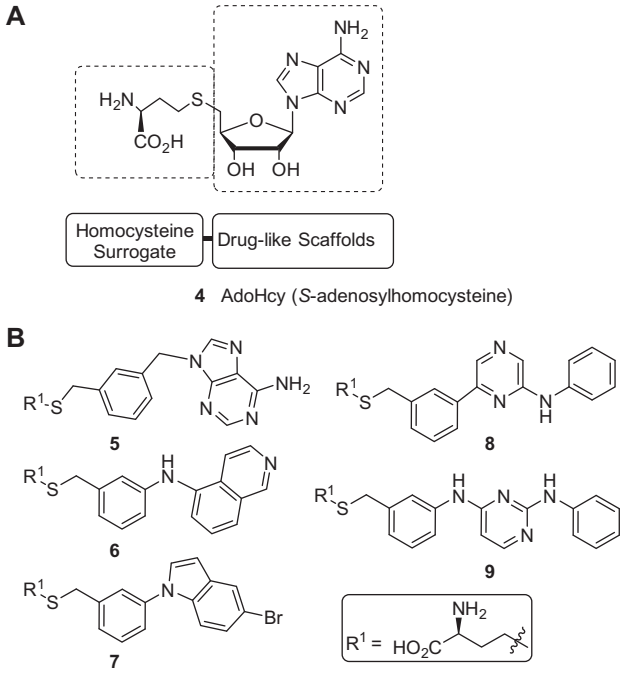

Figure 2. (A) Schematic for the 'biased-privileged' scaffold based strategy to develop KMTase inhibitors. (B) Compounds designed and tested.

2. Results and discussion

We generated a handful of compounds in which homocysteine was appended to 'privileged' chemical scaffolds, which are commonly found in drugs (e.g., kinase inhibitors) (Fig. 2B). Briefly, N-alkylation, palladium-catalyzed Suzuki coupling and copper catalyzed Buchwald couplings were used to obtain compounds **5**–**9**.[28]

We tested their activities against the KMTase, SET7, a well-studied member of this enzyme family. Recombinant SET7 (residues 52–366) was expressed in bacteria as a GST-fusion and purified as previously described.[20,29] Compounds were tested using an ELISA assay in which biotin-conjugated histone H3 peptide (H31-20-cys-biotin) was immobilized on multi-well plates and methylation detected using an antibody that recognizes the monomethylated lysine-4 of histone H3. This assay was based on the method reported by Kubicek et al.[15] Compound **7** was the only active compound, revealing modest activity (~12% inhibition at 40 μM), while all others tested were inactive (Fig. 3). Encouraged by these data, we generated analogs of **7**.

As a first step, we focused on the homocysteine portion of compound **7**, with the goal to reduce the α-amino acid character. We generated γ-butyric acid and meta-benzoic acid substituted versions of **7** using a Buchwald coupling and substitution reactions (Scheme 1A). We found that compounds **10** and **11** were more potent inhibitors of SET7 than **7**. As compound **11** was the most potent, we retained the *meta*-benzoic acid moiety for subsequent analysis. We next examined how changes in the substitutions of the indole impacted activity. We found that Br-substitution at the 4-position (**12**) of the indole increased potency and replacing the Br with a phenyl group (**13**) was even more effective (Scheme 1B). We then examined whether the thioether functionality could be replaced by a secondary amine (**14**), as it would reduce molecular weight and lipophilicity. In addition, this replacement would decrease the likelihood of inhibitor decomposition via oxidation. Gratifyingly, compounds **13** and **14** had similar potencies, yielding ~50–60% inhibition of SET7 at 40 μM.

We next examined whether additional modifications of the 4-phenyl appended to the indole in **14** improved potency. A carboxylic acid at the *para*-position (**15**) of the phenyl ring greatly suppressed activity, while a trifluoromethyl group (**19**) enhanced efficacy. Other substitutions did not lead to further improvements (Schemes 1C and 2A), making compound **19** the best compound in this series. We then examined whether modification of the indole moiety itself impacted the activity of compounds in this series. To this end, we generated compounds **20**–**24** (Scheme 2B), in which the indole in compound **19** was replaced by pyrrolo-pyrimidine (**20**) and benzimidazole (**21**). As we could not readily access 7-aza-indole and 2-indazole analogs for the precise substitution pattern in compound **19**, we generated analogs (**22**–**24**) in which

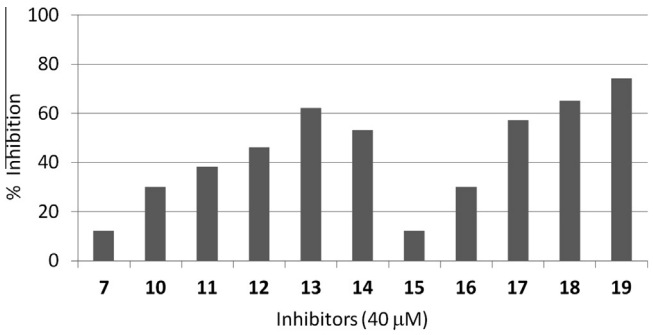

Figure 3. Potency comparison of Indole scaffolds based inhibitors against SET7 in ELISA; inhibition studies were performed with 40 μM inhibitors and DMSO as control ($n \geqslant 2$).

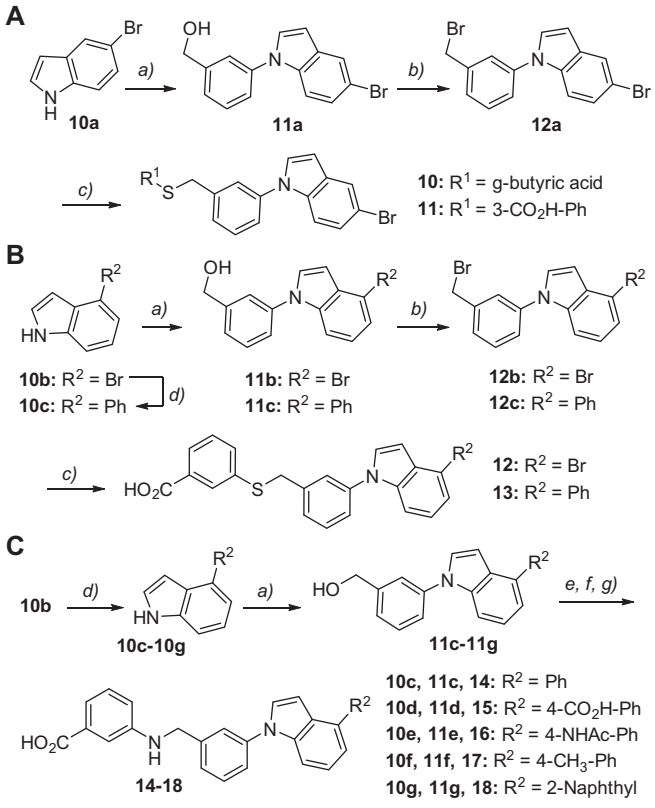

Scheme 1. Synthesis scheme for compounds **10**–**18**. Reagents and conditions: (a) (3-iodophenyl)methanol, 1,4-dioxane, CuI, K_3PO_4, *trans*-*N*,*N*′-dimethylcyclohexane-1,2-diamine, 100 °C, 24 h; (b) CBr_4, PPh_3, DMF, 25 °C, 24 h; (c) R^1SH, NaOH, 100 °C, 5 min, THF, 25 °C, 16 h; (d) $ArB(OH)_2$, 1,4-dioxane, Pd-catalyst, K_2CO_3, 100 °C, 24 h; (e) pyridinium dichromate, CH_2Cl_2, 23 °C, 24 h; (f) 3-aminobenzoic acid, isopropanol, reflux, 4 h; and (g) $NaBH_3CN$, AcOH, acetonitrile, 23 °C, 24 h.

the indole was substituted at the 5-position. Testing revealed that compound **19** remained the most potent compound in the series, with indole being the favoured heterocycle (Fig. 4).

We next focused on the other aromatic rings in compound **20**. Altering the position of the secondary amine (**25**) linking the benzoic acid to the central phenyl ring, or replacing the central phenyl ring with a thiophene (**26**), reduced inhibitor potency. Finally, changes in the benzoic acid moiety (**27**–**35**) also did not yield compounds that were more potent than **19** (Fig. 4).

Figure 5 summarizes our SAR data, with the modifications that improved (+), reduced (−) or did not significantly alter (=) inhibitor activity are indicated. As compound **19** was the best inhibitor of SET7 based on 'biased-privileged' scaffolds, we named it SETin-1. Analysis of dose-dependent inhibition of SET7 activity using an ELISA-based assay yielded an IC_{50} of 10 μM (see Supporting information, Fig. S1). In addition, we analyzed SETin-1's potency using a scintillation proximity assay (SPA), which was designed based on published work,[19,30] as it allowed for homogenous reaction conditions. This assay yielded a comparable IC_{50} of ≈22 μM (Fig. 6A). As we expect these compounds to be active against other KMTases, we generated recombinant G9a, based on literature precedent.[31] As shown in Figure 6B, SETin-1 inhibited this KMTase with comparable potency (IC_{50}: 26.4 ± 4.9 μM) (Fig 6B).

To exclude the possibility that SETin-1 inhibited KMTase activity via an aggregation-type mechanism, we analyzed inhibitor potency at different enzyme concentrations. An unchanged IC_{50} has been recently reported to most reliably indicate that an inhibitor that is not an 'aggregator'.[32] Therefore, we determined IC_{50} values at three different enzyme concentrations (10, 50, and 100 nM). As the IC_{50} was similar under these different conditions (Fig. 6A), we can exclude the possibility SETin-1 inhibits KMTases via such a non-specific mechanism.

3. Conclusion

Our data suggests that our approach, in which we bias drug-like 'privileged' scaffolds with a fragment of an enzyme's cofactor that is known to make important contacts in the binding pocket, can be effective in developing inhibitors. SETin-1 was obtained by testing a handful of compounds and a focused SAR analysis. Improving the potency of this compound will likely require structural studies that should reveal how this compound binds the enzyme. We predict that inhibitors in this series should inhibit KMTases, other that Set7 and G9a. It is also possible that once structural data becomes available, the inhibitors can be modified (or 'bumped') so that they inhibit KMTases with compensatory mutations (or 'holes'). It is likely that these compounds would serve as useful tools to examine KMTase function and the contributions on histone methylation to chromosome biology.

4. Experimental

4.1. General synthesis information

Reactions were run in capped 1 dram vials (4 mL) stirred with Teflon®-coated magnetic stir bars. Moisture- and air-sensitive reactions were performed in flame-dried round bottom flasks, fitted with rubber septa or glass gas adapters, under a positive pressure of nitrogen. Concentration of solvents was accomplished by rotary evaporation using a Büchi rotary evaporator, equipped with a dry ice-acetone condenser, at 5–75 mm Hg at temperatures between 35 and 50 °C. Analytical TLC was performed using Whatman 250 micron aluminum backed UV F_{254} pre-coated silica gel flexible plates. Proton nuclear magnetic resonance spectra (^{1}H NMR) were recorded on Bruker DPX 400 or 600 MHz nuclear magnetic resonance spectrometers. Chemical shifts for ^{1}H NMR spectra are reported as δ in units of parts per million (ppm) relative to tetramethylsilane (δ 0.0) using the residual solvent signal as an internal standard or tetramethylsilane itself: chloroform-*d* (δ 7.26, singlet), dimethylsulfoxide-d_6 (δ 2.50, quintet), methanol-d_4 (δ 3.30, quintet), and deuterium oxide-d_2 (δ 4.80, singlet). Liquid chromatography mass spectral analyses were obtained using a Waters MicroMassZQ mass spectrometer, with an electron spray ionization (ESI) probe, connected to a Waters 2795 HT Separation Module Alliance HT HPLC system running MassLynx (V4.0).

4.2. Synthetic procedures and characterization of compounds

4.2.1. (*S*)-4-((3-((6-Amino-9*H*-purin-9-yl)methyl)phenyl)methylthio)-2-aminobutanoic acid (5)

Alkylation of adenine using α,α′-dichloro-*m*-xylene (195.0 mg, 1.10 mmol) and purification by crystallization (methanol-ethyl acetate) afforded 9-(3-(chloromethyl)benzyl)-9*H*-purin-6-amine (178.5 mg, 56% yield) as white powder; ^{1}H NMR (400 MHz, DMSO-d_6): δ 8.63 (s, 1H), 7.41–7.23 (m, 4H), 5.39 (s, 2H), 4.73 (s, 2H). Bromine displacement by L-homocysteine thiolate using 9-(3-(chloromethyl)benzyl)-9*H*-purin-6-amine (66.9 mg, 0.244 mmol), ethanol (0.20 mL), sodium iodide (36.6 mg, 0.244 mmol), stirred at 110 °C for 15 min and purification by reverse phase HPLC (gradient run: 5% B for 3 min then ramp to 75% B over 30 min) afforded compound **5**, (15.8 mg, 17% yield) as clear film and as trifluoroacetate salt; ^{1}H NMR (400 MHz,

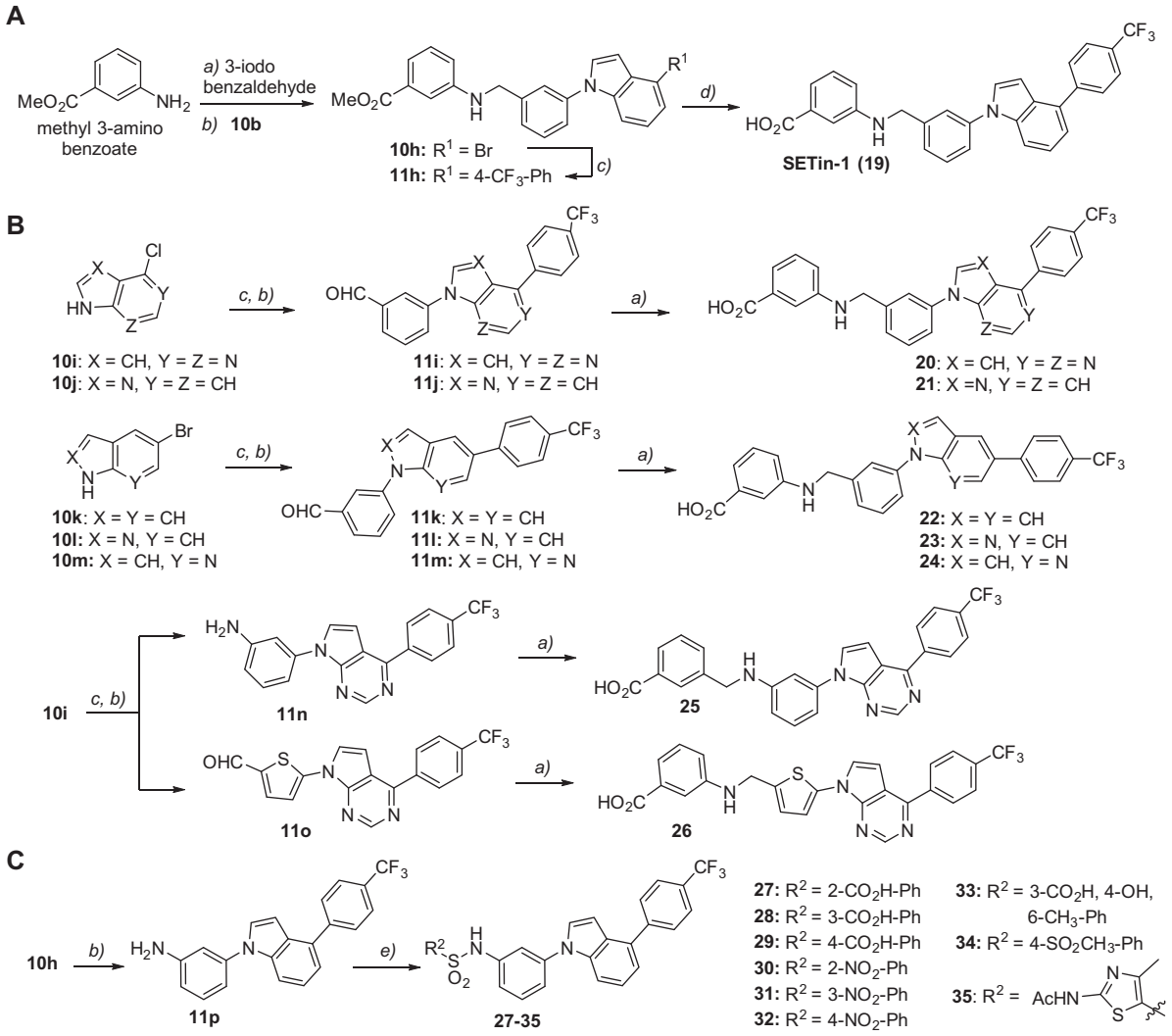

Scheme 2. General Synthesis scheme for compounds **19**–**35**: (A) 4-CF_3-phenyl substitution on indole. (B) Inhibitors containing similar drug-like heterocycles. (C) General synthetic scheme for sulfonamide compounds. Reagents and conditions: (a) $ArNH_2$ (CO_2H) or ArCHO (CO_2H), $NaBH_3CN$, *p*-TSA, MeOH: CH_2Cl_2 (1:1), 25 °C, 24 h; (b) Het-Br or ArI, 1,4-dioxane, CuI, K_3PO_4, *trans-N,N′*-dimethylcyclohexane-1,2-diamine, 100 °C, 24 h; (c) 4-(trifluoromethyl)phenylboronic acid, 1,4-dioxane, Pd-catalyst, K_2CO_3, 100 °C, 24 h; (d) $LiOH{\cdot}H_2O$, THF/MeOH/H_2O (1:1:1), 25 °C, 24 h; and (e) $ArSO_2Cl$, pyridine, CH_2Cl_2, 25 °C, 24 h.

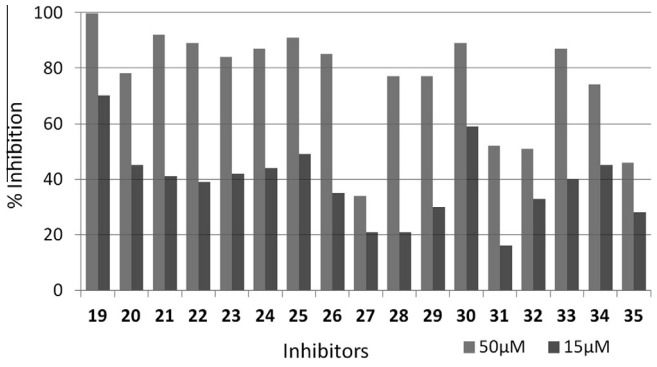

Figure 4. Inhibitory effect of CF_3-substituted heteroaryl groups and sulfonamides on SET7 activity in SPA, 50 and 15 μM of inhibitors and DMSO as control ($n \geqslant 2$).

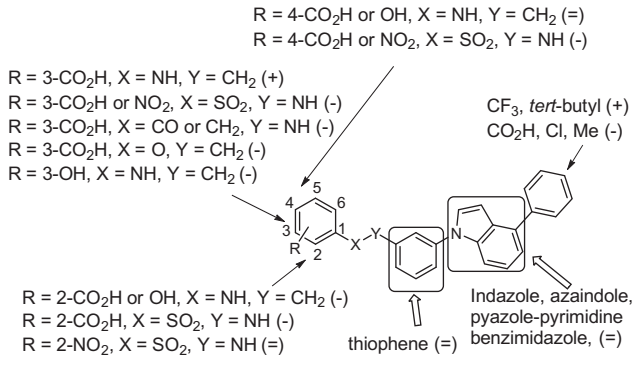

Figure 5. SAR summary for drug-like scaffold inhibitors of KMTases.

D_2O): δ 8.47 (s, 1H), 8.44 (s, 1H), 7.45–7.30 (m, 4H), 5.57 (s, 2H), 4.13 (t, *J* = 6.4 Hz, 1H), 3.82 (s, 2H), 2.62 (t, *J* = 7.4 Hz, 2H), 2.21–2.09 (m, 2H). Calcd mass for $C_{17}H_{20}N_6O_2S$: 372.14; LRMS (ESI) *m*/*z* $[M+H]^+$ = 373.43.

4.2.2. (*S*)-4-(3-(Isoquinolin-5-ylamino)benzylthio)-2-aminobutanoic acid (6)

Buchwald coupling using 5-aminoisoquinoline (175.8 mg, 1.22 mmol), stirred at 100 °C for 14 h and purified by chromatography (12 g silica gel, 60% ethyl acetate–petroleum ether to 100%

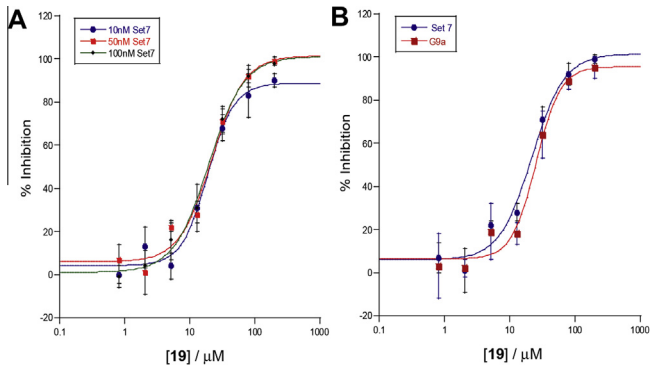

Figure 6. (A) Dose response curve of compound **19** at increasing concentrations of SET7 in SPA (IC_{50}: 10 nM SET7 = 19.0 ± 1.0 μM; 50 nM SET7 = 22.5 ± 1.2 μM, 100 nM SET7 = 19.5 ± 1.5 μM). (B) Dose–response curves for **19** against SET7 or G9a, IC50's: SET7 = 22.5 ± 1.2 μM; G9a = 26.4 ± 4.9 μM.

ethyl acetate) to afford (3-(isoquinolin-5-ylamino)phenyl)methanol (18.3 mg, 6% yield) as pale orange film; ^{1}H NMR (400 MHz, $CDCl_3$): δ 9.18 (s, 1H), 8.42 (d, J = 5.9 Hz, 1H), 7.72 (d, J = 5.9 Hz, 1H), 7.60 (d, J = 7.7 Hz, 1H), 7.52–7.47 (m, 2H), 7.25 (t, J = 7.5 Hz, 1H), 7.05 (s, 1H), 6.94 (t, J = 8.2 Hz, 2H), 6.11 (s, 1H), 4.65 (s, 2H). Bromination using (3-(isoquinolin-5-ylamino)phenyl)methanol (18.3 mg, 0.073 mmol), and purified very quickly by chromatography (10 g silica gel, 0–2% methanol–dichloromethane) to afford *N*-(3-(bromomethyl)phenyl)isoquinolin-5-amine as pale yellow film, which was not fully concentrated to avoid the intermolecular reation. Bromine displacement by L-homocysteine thiolate using *N*-(3-(bromomethyl)phenyl) isoquinolin-5-amine, EtOH (0.4 mL), stirred at room temperature for 16 h, and purification by reverse phase HPLC (gradient run: 5% B for 3 min then ramp to 75% B over 30 min) afforded compound **6**, (8.6 mg, 32% yield over two steps) as bright yellow film and as trifluoroacetate salt; ^{1}H NMR (400 MHz, D_2O): δ 9.60 (s, 1H), 8.54 (d, J = 6.8 Hz, 1H), 8.46 (d, J = 6.8 Hz, 1H), 8.07 (d, J = 7.0 Hz, 1H), 7.95–7.90 (m, 2H), 7.37 (t, J = 7.9 Hz, 1H), 7.11 (s, 1H), 7.06 (d, J = 6.8 Hz, 2H), 4.14 (t, J = 6.1 Hz, 1H), 3.78 (s, 1H), 2.69 (t, J = 7.4 Hz, 2H), 2.29–2.17 (m, 2H). Calcd mass for $C_{20}H_{21}N_3O_2S$: 367.14; LRMS (ESI) m/z $[M+H]^+$ = 368.40.

4.2.3. (*S*)-4-(3-(5-Bromo-1*H*-indol-1-yl)benzylthio)-2-aminobutanoic acid (7)

Buchwald coupling using 5-bromoindole (282.0 mg, 1.438 mmol), stirred at 90 °C for 6.5 h (in order to avoid the polymerization and bromide to iodide exchange), and purified by chromatography (12 g silica gel, 0–40% ethylacetate–petroleum ether) to afford (3-(5-bromo-1*H*-indol-1-yl)phenyl)methanol (284.7 mg, 67% yield) as clear film; ^{1}H NMR (400 MHz, $CDCl_3$): δ 7.77 (s, 1H), 7.48–7.22 (m, 7H), 6.58 (d, J = 2.7 Hz, 1H), 4.75 (d, J = 5.3 Hz, 2H), 1.81 (t, J = 5.5 Hz, 1H). Bromination using (3-(5-bromo-1*H*-indol-1-yl)phenyl)methanol (276.9 mg, 0.916 mmol), and purification by chromatography (15 g silica gel, 0–5% ethyl acetate–petroleum ether) afforded 5-bromo-1-(3-(bromomethyl)phenyl)-1*H*-indole (261.4 mg, 78% yield) as pink yellow viscous oil; ^{1}H NMR (400 MHz, $CDCl_3$): δ 7.80 (s, 1H), 7.50–7.28 (m, 7H), 6.62 (d, J = 2.9 Hz, 1H), 4.53 (s, 2H). Bromine displacement by L-homocysteine thiolate using 5-bromo-1-(3-(bromomethyl)phenyl)-1*H*-indole (11.3 mg, 0.031 mmol), ethanol (0.4 mL), stirred at 110 °C for 1 h, and purification by reverse phase HPLC (gradient run: 5% B for 3 min then ramp to 75% B over 30 min) afforded compound **7**, (5.3 mg, 32% yield) as clear film and as trifluoroacetate salt; ^{1}H NMR (400 MHz, D_2O): δ 7.77 (s, 1H), 7.52–7.37 (m, 6H), 7.27 (d, J = 8.8 Hz, 1H), 6.64 (d, J = 2.7 Hz, 1H), 4.07 (t, J = 6.2 Hz, 1H), 3.88 (m, 2H), 2.66 (t, J = 7.5 Hz, 2H), 2.27–2.18 (m, 1H), 2.15–2.05 (m, 1H). Calcd mass for $C_{19}H_{19}BrN_2O_2S$: 418.04; LRMS (ESI) m/z $[M+H]^+$ = 419.24/421.22 (bromine pattern).

4.2.4. (*S*)-4-(3-(6-(Phenylamino)pyrazin-2-yl)benzylthio)-2-aminobutanoic acid (8)

Aniline (265.7 mg, 2.85 mmol) and 2,6-dichloropyrazine (427.2 mg, 2.87 mmol) were dissolve in *n*-butanol (2.0 mL), and 4.0 M hydrochloric acid in 1,4-dioxane (2 mL) was added. The mixture was heated to 120 °C for 96 h, poured in water (30 mL), extracted with ethyl acetate (30 mL), the organic layer was washed with saturated aqueous sodium bicarbonate solution (30 mL) and brine (25 mL), concentrated and purified by chromatography (30 g silica gel, 0.5–1.0% ethyl acetate–dichloromethane) to afford 6-chloro-*N*-phenylpyrazin-2-amine (225.9 mg, 38% yield) as a dark yellow semi-solid; ^{1}H NMR (400 MHz, $CDCl_3$): δ 8.10 (s, 1H), 7.97 (s, 1H), 7.40–7.35 (m, 4H), 7.17–7.12 (m, 1H), 6.74 (s, 1H); Calcd mass for $C_{10}H_8ClN_4$: 205.04; LRMS (ESI) m/z $[M+H]^+$ = 206.20. Suzuki coupling using 6-chloro-*N*-phenylpyrazin-2-amine (47.7 mg, 0.232 mmol), 3-hydroxymethylphenylboronic acid (39.0 mg, 0.257 mmol) and purified by chromatography (4 g silica gel, 0–10% methanol–dichloromethane) to afford (3-(6-(phenylamino)pyrazin-2-yl)phenyl)methanol (48.6 mg, 76% yield) as a yellow solid; Calcd mass for $C_{17}H_{15}N_4O$: 277.12; LRMS (ESI) m/z $[M+H]^+$ = 278.29. Bromination using (3-(6-(phenylamino) pyrazin-2-yl)phenyl)methanol (48.6 mg, 0.175 mmol), 1:1 dichloromethane–tetrahydrofuran (2.0 mL) as solvent, and purified by chromatography (12 g silica gel, 25–80% ethyl acetate–petroleum ether) to afford 6-(3-(bromomethyl)phenyl)-*N*-phenylpyrazin-2-amine which was used quickly for the next step. Bromine displacement by L-homocysteine thiolate using 6-(3-(bromomethyl)phenyl)-*N*-phenylpyrazin-2-amine (16.6 mg, 0.49 mmol), 1:1 tetrahydrofuran–water (0.20 mL), stirred at 55 °C for 13 h, and purification by reverse phase HPLC (gradient run: 50% B for 3 min then ramp to 70% B over 30 min) afforded compound **8**, (8.5 mg, 34% yield) as a pale yellow' solid and as the trifluoroacetate salt; ^{1}H NMR (400 MHz, DMSO-d_6): δ 9.60 (s, 1H), 8.54 (s, 1H), 8.20 (s, 1H), 8.08 (s, 1H), 7.96 (d, J = 7.3 Hz, 1H), 7.81 (d, J = 7.9 Hz, 2H), 7.50–7.34 (m, 4H), 6.99 (t, J = 7.3 Hz, 1H), 3.84 (s, 2H), 2.58 (t, J = 7.3 Hz, 2H), 2.10–2.01 (m, 1H), 1.90–1.83 (m, 1H). Calcd mass for $C_{21}H_{22}N_4O_2S$: 394.15; LRMS (ESI) m/z $[M+H]^+$ = 395.42.

4.2.5. (*S*)-4-(3-(2-(Phenylamino)pyrimidin-4-ylamino)benzylthio)-2-aminobutanoic acid (9)

Amine displacement using ethyl 3-aminobenzoate (352.0 mg, 2.13 mmol), 2,4-dichloropyrimidine (318.0 mg, 2.13 mmol), diisopropylamine (0.742 mL, 4.26 mmol), and ethylene glycol (1.0 mL), was stirred at 130 °C for 6 h. Instead of working up the reaction, 4.0 M hydrochloride acid in 1,4-dioxane (0.55 mL, 2.20 mmol), and aniline (0.20 mL, 2.19 mmol) were added, and the mixture was stirred at 120 °C for 11 h. The reaction was poured into water (20 mL), extracted with 1:1 ethyl acetate–petroleum ether (2 × 30 mL), the organic layers were sequentially washed with water (20 mL) and brine (20 mL), concentrated, and purified by chromatography (12 g silica gel, 5–70% ethyl acetate–petroleum ether) to afford ethyl-3-(2-(phenylamino)pyrimidin-4-ylamino)benzoate (crude weight 260 mg) as a mixture of compounds used without further purification. Crude ethyl-3-(2-(phenylamino)pyrimidin-4-ylamino)benzoate was dissolved in dichloromethane (20 mL) and cooled to 0 °C. A solution of 1.0 M diisobutylaluminum hydride in toluene (3.0 mL, 3.00 mmol) was added slowly in three portions every 20 min over 1 h. The reaction was deemed complete by TLC (80% ethyl acetate–petroleum ether). The reaction was quenched with methanol (1.2 mL), ground anhydrous sodium sulfate (8.5 g), water (10.8 mL), and Celite® (75 mL), stirred vigorously for 30 min, filtered, washed with dichloromethane, concentrated

and purified by chromatography (12 g silica gel, 0–10% methanol–dichloromethane) to afford (3-(2-(phenylamino)pyrimidin-4-ylamino)phenyl)methanol (58.5 mg, 9% yield) as a white foam; ^{1}H NMR (400 MHz, $CDCl_3$): δ 9.03 (d, J = 5.9 Hz, 1H), 7.56 (d, J = 7.9 Hz, 2H), 7.40 (s, 1H), 7.35–7.26 (m, 4H), 7.13–7.10 (m, 2H), 7.02 (t, J = 7.3 Hz, 1H), 6.69 (s, 1H), 6.16 (d, J = 5.9 Hz, 1H), 4.68 (s, 2H); Calcd mass for $C_{17}H_{16}N_4O$: 292.13; LRMS (ESI) m/z $[M+H]^+$ = 293.41. Bromination using (3-(2-(phenylamino)pyrimidin-4-ylamino)phenyl)methanol (58.5 mg, 0.20 mmol), 1:1 dichloromethane–tetrahydrofuran (2.0 mL) as solvent, and purified by chrornatography (4 g silica gel, 10% ethyl acetate–petroleum ether to 100% ethyl acetate) to afford N4-(3-(bromomethyl)phenyl)-N2-phenylpyrimidine-2,4-diamine (38.8 mg, 55% yield) as a clear film; ^{1}H NMR (400 MHz, $CDCl_3$): δ 8.06 (d, J = 5.7 Hz, 1H), 7.56 (d, J = 7.7 Hz, 2H), 7.46 (s, 1H), 7.38 (s, 1H), 7.33–7.25 (m, 4H), 7.14 (d, J = 6.6 Hz, 1lH), 7.03 (t, J = 7.3 Hz, 1H), 6.86 (s, 1H), 6.16 (d, J = 5.9 Hz, 1H), 4.44 (s, 2H); Calcd mass for $C_{17}H_{15}BrN_4$: 354.05; LRMS (ESI) m/z $[M+H]^+$ = 355.38/357.41 (bromine pattern). Bromine displacement by L-homocysteine thiolate using N4-(3-(bromomethyl)phenyl)-N2-phenylpyrimidine-2,4-diamine (19.4 mg, 0.0546 mmol), 3:1 ethanol–water (0.40 mL), stirred at 55 °C for 1.5 h, and purification by reverse phase HPLC (gradient run: 15% B for 3 min then ramp to 100% B over 30 min) afforded compound **9**, (13.9 mg, 49% yield) as a clear film and as the trifluoroacetate salt; ^{1}H NMR (400 MHz, CD_3OD): δ 7.76 (d, J = 7.0 Hz, 1H), 7.56 (s, 1H), 7.50–7.40 (m, 5H), 7.30–7.25 (m, 2H), 7.18 (d, J = 7.5 Hz, 1H), 6.40 (d, J = 7.1 Hz, 1H), 3.79 (t, J = 6.2 Hz, 1H), 3.70 (s, 2H), 2.55 (t, J = 7.6 Hz, 2H), 2.18–2.03 (m, 1H). Calcd mass for $C_{21}H_{23}N_5O_2S$: 409.16; LRMS (ESI) m/z $[M+H]^+$ = 410.42.

4.2.6. 4-(3-(5-Bromo-1*H*-indol-1-yl)benzylthio)butanoic acid (10)

A 1.5 M solution of γ-butyrate thiolate was prepared by dissolving γ-butyrothiolactone (30.0 mg, 0.296 mmol) into 2.96 M aqueous sodium hydroxide (0.195 mL, 0.577 mmol) at 100 °C for 5 min. A 0.18 M solution of intermediate 5-bromo-1-(3-(bromomethyl)phenyl)-1*H*-indole (37.3 mg, 0.102 mmol) in tetrahydrofuran (0.57 mL) was added to the aqueous solution, and stirred at room temperature for 16 h. Upon completion, the reaction was poured into 1.0 M aqueous hydrochloric acid (20 mL), extracted with 1:1 ethyl acetate–petroleum ether (30 mL), the organic layer was washed with brine (10 mL), concentrated, and purified by chromatography (4 g silica gel, 0–7% methanol–dichloromethane). A portion of this material was filtered (PALL Life Sciences, Acrodisc® Premium, 25 mm syringe filters with 0.45 micron GHP membrane, catalog# AP-4560T), purified by reverse phase HPLC (VYDAC C18, 11 × 250 mm column; flow rate 6 mL/min; UV detection: 254 nm; solvent A: water with 0.1% ammonium hydroxide, solvent B: acetonitrile; gradient run: 5% B for 3 min then ramp to 40% B over 25 min), and neutralized to afford compound **10**, (2.9 mg) as a clear film; ^{1}H NMR (400 MHz, $CDCl_3$): δ 7.80 (s, 1H), 7.52–7.37 (m, 7H), 6.61 (d, J = 2.9 Hz, 1H), 3.78 (s, 2H), 2.54 (t, J = 7.1 Hz, 2H), 2.47 (t, J = 7.1 Hz, 2H), 1.91 (quint, J = 7.1 Hz, 2H). Calcd mass for $C_{19}H_{18}BrNO_2S$: 403.02; LRMS (ESI) m/z $[M-H]^-$ = 402.22/404.22 (bromine pattern).

4.2.7. 3-(3-(5-Bromo-1*H*-indol-1-yl)benzylthio)benzoic acid (11)

A 1.5 M solution of 3-benzoate thiolate was prepared by dissolving 3-mercaptobenzoic acid (31.3 mg, 0.203 mmol) into 2.96 M aqueous sodium hydroxide (0.135 mL, 0.40 mmol) at 100 °C for 5 min. A 0.18 M solution of intermediate 5-bromo-1-(3-(bromomethyl)phenyl)-1*H*-indole (37.3 mg, 0.102 mmol) in tetrahydrofuran (0.57 mL) was added to the aqueous solution, and stirred at room temperature for 16 h. Upon completion, the reaction was poured into 1.0 M aqueous hydrochloric acid (20 mL), extracted with 1:1 ethyl acetate–petroleum ether (30 mL), the organic layer was washed with brine (10 mL), concentrated, and purified by chromatography (4 g silica gel, 0–10% methanol–dichloromethane). A portion of this material was filtered (PALL Life Sciences, Acrodisc® Premium, 25 mm syringe filters with 0.45 micron GHP membrane, catalog# AP-4560T), purified by reverse phase HPLC (VYDAC Cl8 , 11 × 250 mm column; flow rate 6 mL/min; UV detection: 254 nm; solvent A: water with 0.1% ammonium hydroxide, solvent B: acetonitrile; gradient run: 5% B for 3 min then ramp to 40% B over 25 min), and neutralized to afford compound **11**, (1.7 mg) as a clear film; ^{1}H NMR (400 MHz, $CDCl_3$): δ 7.88 (s, 1H), 7.86 (d, J = 12.99 Hz, 1H), 7.77 (d, J = 7.68 Hz, 1H), 7.60–7.65 (m, 2H), 7.49–7.54 (m, 2H), 7.40–7.47 (m, 3H), 6.68 (d, J = 3.29 Hz, 1H), 4.41 (s, 2H). Calcd mass for $C_{22}H_{16}BrNO_2S$: 437.01; LRMS (ESI) m/z $[M-H]^-$ = 436.21/438.28 (bromine pattern).

4.2.8. 3-(3-(4-Bromo-1*H*-indol-1-yl)benzylthio)benzoic acid (12)

Following the same procedure used to synthesize (**7**), but using 4-bromoindole in the Buchwald coupling step, affords compound **12**; ^{1}H NMR (400 MHz, DMSO-d_6): δ 7.88 (s, 1H), 7.77 (d, J = 8.27 Hz, 1H), 7.71 (d, J = 3.30 Hz, 1H), 7.64 (d, J = 7.78 Hz, 1H), 7.54–7.50 (m, 2H), 7.47–7.41 (m, 3H), 7.35 (d, J = 7.57 Hz, 1H), 7.30 (d, J = 8.41 Hz, 1H), 7.09 (t, J = 7.85 Hz, 1H), 6.65 (d, J = 3.36 Hz, 1H), 4.41 (s, 2H). Calcd mass for $C_{22}H_{16}BrNO_2S$: 437.01; LRMS (ESI) m/z $[M-H]^-$ = 436/438 (bromine pattern).

4.2.9. 3-(3-(4-Phenyl-1*H*-indol-1-yl)benzylthio)benzoic acid (13)

Suzuki coupling using 4-bromoindole (938.8 mg, 4.79 mmol), phenylboronic acid (603.1 mg, 4.95 mmol), and purified by chromatography (40 g silica gel, 0–35% ethyl acetate–petroleum ether) to afford 4-phenyl-1*H*-indole (622.7 mg, 67% yield) as a pale purple viscous oil; Calcd mass for $C_{14}H_{11}N$: 193.09; LRMS (ESI) m/z $[M+H]^+$ = 194.28. Buchwald coupling using 4-phenyl-1*H*-indole (104.4 mg, 0.54 mmol), and purification by chromatography (12 g silica gel, 0–40% ethyl acetate–petroleum ether) afforded (3-(4-phenyl-1*H*-indol-1-yl)phenyl)methanol (104.8 mg, 65% yield) as a white crystalline solid; ^{1}H NMR (400 MHz, $CDCl_3$): δ 7.71 (*d*, J = 7.5 Hz, 2H} 7.55–7.44 (m, 6H), 7.40–7.35 (m, 3H), 7.29 (t, J = 7.8 Hz, 1H), 7.23 (d, J = 7 .0 Hz, 1H), 6.84 (d, J = 3.1 Hz, 1H), 4.19 (s, 2H), 1.85 (s, 1H); Calcd mass for $C_{21}H_{17}NO$: 299.13; LRMS (ESI) m/z $[M+H]^+$ = 300.41. Bromination using (3-(4-phenyl-1*H*-indol-1-yl)phenyl)methanol (104.8 mg, 0.35 mmol), and purification by chromatography (4 g silica gel, 0–25% ethyl acetate–petroleum ether) afforded 1-(3-(bromomethyl)phenyl)-4-phenyl-1*H*-indole (112.5 mg, 89% yield) as a clear film; ^{1}H NMR (400 MHz, $CDCl_3$): δ 8.71 (d, J = 7.3 Hz, 2H), 7.56–7.45 (m, 6H), 7.40–7.36 (m, 3H), 1.31 (t, J = 7.7 Hz, 1H), 7.24 (d, J = 7.7 Hz, 1H), 6.85 (d, J = 2.9 Hz, 7H), 4.54 (s, 2H). A 1.03 M solution of 3-benzoate thiolate was prepared from 3-mercaptobenzoic acid and 2.06 M aqueous sodium hydroxide as above. The solution of 3-benzoate thiolate (0.040 mL, 0.0412 mmol) was added to a solution of intermediate 1-(3-(bromomethyl)phenyl)-4-phenyl-1*H*-indole (14.1 mg, 0.0389 mmol) in tetrahydrofuran (0.5 mL), and the mixture was stirred at room temperature for 16 h. Upon completion, the reaction was diluted with 1.0 M aqueous hydrochloric acid (1 mL), extracted with ethyl acetate (2 mL), the organic layer was washed with brine (10 mL), concentrated, and purified by chromatography (4 g silica gel, 0–5% methanol–dichloromethane) to afford compound **13**, (16.6 mg, 98% yield) as a clear film; ^{1}H NMR (400 MHz, DMSO-d_6): δ 7.89 (s, 1H), 7.79 (d, J = 7.68 Hz, 1H), 7.69–7.62 (m, 4H), 7.58–7.50 (m, 4H), 7.48–7.38 (m, 4H), 7.31 (d, J = 7.87 Hz, 1H), 7.24 (t, J = 8.05 Hz, 1H), 7.20 (d, J = 6.59 Hz, 1H), 6.76 (d, J = 3.29 Hz, 1H), 4.43 (s, 2H). Calcd mass for $C_{28}H_{21}NO_2S$: 435.13; LRMS (ESI) m/z $[M-H]^-$ = 434.20.

4.2.10. 3-(3-(4-Phenyl-1*H*-indol-1-yl)benzylamino)benzoic acid (14)

A solution of (3-(4-phenyl-1*H*-indol-1-yl)phenyl)methanol was dissolved in dichloromethane and treated with pyridinium dichromate to form the aldehyde (Swern conditions also work). The mixture was filtered through Celite and the dark orange solution was concentrated, and purified directly by chromatography (silica gel, 10–75% ethyl acetate–hexanes) to afford 3-(4-phenyl-1*H*-indol-1-yl)benzaldehyde; ^{1}H NMR (300 MHz, $CDCl_3$): δ 8 10.12 (s, 1H), 8.06 (d, 1H), 7.90–7.80 (m, 2H), 7.75–7.70 (m, 3H), 7.60–7.45 (m, 3H), 7.60–7.45 (m, 3H), 7.20–7.10 (m, 1H), 6.90 (d, 1H). 3-(4-phenyl-1*H*-indol-1-yl)benzaldehyde (29.75 mg, 0.1 mmol) was dissolved in isopropanol (0.3 mL, 0.33 M) and 3-aminobenzoic acid (13.7 mg, 0.1 mmol) was added. The reaction was heated at reflux for 2–4 h and concentrated to remove isopropanol. The residue was dissolved in acetonitrile (0.3 mL) then acetic acid (12 μL, 0.2 mmol) and solid sodium cyanoborohydride (7 mg, 0.11 mmol) were added at 23 °C. The reaction was stirred overnight at 23 °C and then quenched with 0.5 M aqueous oxalic acid. The mixture was stirred at 23 °C for 30 min, poured into water, extracted with 1:1 ethyl acetate–hexane, filtered and concentrated. Purification by chromatography (4 g silica gel, 0–5% methanol–dichloromethane with 0.5% acetic acid) afforded compound **14** (2 mg) as a clear film; ^{1}H NMR (400 MHz, $CDCl_3$): δ 7.70 (d, J = 7.68 Hz, 2H), 7.55 (s, 1H), 7.51–7.43 (m, 6H), 7.41–7.35 (m, 4H), 7.29–7.21 (m, 3H), 6.87 (dd, J = 5.85, 2.20 Hz, 1H), 6.83 (d, J = 3.29 Hz, 1H), 4.50 (s, 2H). Calcd mass for $C_{28}H_{22}N_2O_2$: 418.17; LRMS (ESI) m/z $[M-H]^-$ = 417.74.

4.2.11. 3-(3-(4-(4-Carboxyphenyl)-1*H*-indol-1-yl)benzylamino)benzoic acid (15)

Following the same procedure used to synthesize (**14**), but using 4-carboxyphenylboronic acid in the Suzuki coupling step, affords compound **15**; ^{1}H NMR (300 MHz , $CDCl_3$+CD_3OD): δ 8.10 (d, 2H), 7.71 (d, 2H), 7.47–7.30 (m, 9H), 7.19–7.12 (m, 3H), 6.77–6.72 (m, 2H), 4.24 (s, 2H). Calcd mass for $C_{29}H_{22}N_2O_4$: 462.16; LRMS (ESI) m/z $[M+Na]^+$ = 485.56.

4.2.12. 3-(3-(4-(4-Acetamidophenyl)-1*H*-indol-1-yl)benzylamino)benzoic acid (16)

Following the same procedure used to synthesize (**14**), but using 4-acetamidophenylboronic acid in the Suzuki coupling step, affords compound **16**; ^{1}H NMR (300 MHz , $CDCl_3$): δ 7.64 (d, 2H), 7.54–7.34 (m, 9H), 7.30–7.07 (m, 3H), 6.86 (dd, 1H), 6.81 (d, 2H), 4.52 (s, 2H), 2.23 (s, 3H). Calcd mass for $C_{30}H_{25}N_3O_3$: 475.19; LRMS (ESI) m/z $[M+Na]^+$ = 498.63.

4.2.13. 3-(3-(4-*p*-Tolyl-1*H*-indol-1-yl)benzylamino)benzoic acid (17)

Following the same procedure used to synthesize (**14**), but using *p*-tolylboronic acid in the Suzuki coupling step, affords compound **17**; ^{1}H NMR (300 MHz , $CDCl_3$): δ 7.61 (d, 2H), 7.46–7.32 (m, 8H), 7.30–7.22 (m, 8H), 6.85–6.84 (m, 2H), 4.50 (s, 2H). Calcd mass for $C_{29}H_{24}N_2O_2$: 432.18; LRMS (ESI) m/z $[M+Na]^+$ = 455.64.

4.2.14. 3-(3-(4-(Naphthalen-2-yl)-1*H*-indol-1-yl)benzylamino)benzoic acid (18)

Following the same procedure used to synthesize (**14**), but using naphthalen-2-ylboronic acid in the Suzuki coupling step, affords compound **18**; ^{1}H NMR (300 MHz , $CDCl_3$): δ 8.17 (s, 1H), 7.80 (m, 4H), 7.55–7.50 (m, 6H), 7.42–7.31 (m, 7H), 6.92–6.89 (m, 2H), 4.52 (s, 2H). Calcd mass for $C_{32}H_{24}N_2O_2$: 468.18; LRMS (ESI) m/z $[M+Na]^+$ = 491.64.

4.2.15. 3-(3-(4-(4-(Trifluoromethyl)phenyl)-1*H*-indol-1-yl)benzylamino)benzoic acid (19)

To a preformed solution of methyl 3-aminobenzoate (500 mg, 3.30 mmol) and 3-iodobenzaldehyde (842 mg, 3.63 mmol) in (1:1) MeOH/CH_2Cl_2 (1.0 M) was added *p*-TSA (624 mg, 3.63 mmol) followed by $NaBH_3CN$ (228 mg, 3.63 mmol) over a period of 5 min at room temperature. The reaction mixture was stirred at room temperature under the nitrogen atmosphere. After completion of the reaction (monitored by TLC), reaction mixture was diluted with ethyl acetate (20 mL) and quenched with water (10 mL), extracted with ethyl acetate (3 × 20 mL), the organic layer was washed with water (20 mL), dried over Na_2SO_4. The solvent was removed under reduced pressure and crude reaction mixture was purified by column chromatography (50 g silica gel, 0–15% ethyl acetate–petroleum ether) to afford methyl-3-(3-iodobenzylamino)benzoate (640 mg, 53% yield) as off white powder; ^{1}H NMR (400 MHz, $CDCl_3$): δ 7.73 (s, 1H), 7.61 (d, J = 7.92 Hz, 1H), 7.40 (d, J = 7.52 Hz, 1H), 7.34–7.29 (m, 2H), 7.22 (t, J = 7.88 Hz, 1H), 7.07 (t, J = 7.69 Hz, 1H), 6.77 (dd, J = 6.05, 2.17 Hz, 1H), 4.32 (s, 2H), 3.89 (s, 3H). Calcd mass for $C_{15}H_{14}INO_2$: 367.01; LRMS (ESI) m/z $[M+H]^+$ = 368.74. To a solution of methyl-3-(3-iodobenzylamino)benzoate (200 mg, 0.544 mmol) and 4-bromoindole (117 mg, 0.599 mmol) in 1,4-dioxane (1.0 M) was added freshly ground potassium phosphate tribasic (254 mg, 1.197 mmol), copper(I) iodide (7.25 mg, 0.038 mmol) and racemic *trans-N,N′*-dimethylcyclohexane-1,2-diamine (12 μL, 0.0816 mmol). The suspension was degassed for 5 min by bubbling nitrogen gas directly into the solution using syringe needle. The reaction vessel was closed tightly and stirred at 100 °C for overnight or until the completion of reaction as judged by TLC. The reaction mixture was filtered through a pad of celite, poured into water (25 mL) and extracted with ethyl acetate (3 × 25 mL), the organic layer was washed with water (20 mL), dried over Na_2SO_4. Excess of Solvent was evaporated under reduced pressure and resulting crude mixture was purified by chromatography (20 g silica gel, 0–15% ethylacetate–petroleum ether) to afford methyl 3-(3-(4-bromo-1*H*-indol-1-yl)benzylamino)benzoate (150 mg, 63% yield) as clear film; ^{1}H NMR (400 MHz, $CDCl_3$): δ 7.49 (t, J = 7.84 Hz, 1H), 7.47 (s, 1H), 7.41 (d, J = 7.66 Hz, 1H), 7.38–7.30 (m, 6H), 7.23 (t, J = 7.86 Hz, 1H), 7.01 (t, J = 7.87 Hz, 1H), 6.80 (dd, J = 6.74, 1.27 Hz, 1H), 6.71 (d, J = 2.94 Hz, 1H), 4.47 (s, 2H), 3.87 (s, 3H). Calcd mass for $C_{23}H_{19}BrN_2O_2$: 435.31; LRMS (ESI) m/z $[M]^+$ = 435.55, 437.34 (bromine pattern). To a solution of methyl 3-(3-(4-bromo-1*H*-indol-1-yl)benzylamino)benzoate (40 mg, 0.092 mmol) and 4-trifluromethylphenyl boronic acid (19.5 mg, 0.101 mmol) in 1,4-dioxane (1.0 M) was added potassium carbonate (25 mg, 0.184 mmol, 2.0 M aqueous solution) followed by palladium catalyst [1, 1′-bis(diphenylphoshphino)ferrocene]-dichloropalladium(II) 1:1 complex with dichloromethane (7.5 mg, 0.0092 mmol). The reaction mixture was degassed for 5 min by bubbling nitrogen gas directly into the solution using syringe needle. The reaction vessel was closed tightly and stirred at 100 °C for overnight or until the completion of reaction as judged by TLC. The reaction mixture was filtered through a pad of silica/celite to remove the catalyst, poured into water (25 mL) and extracted with ethyl acetate (3 × 25 mL), the organic layers were washed with water (20 mL), dried over Na_2SO_4, concentrated under reduced pressure and purified by chromatography (5 g silica gel, 0–15% ethyl acetate–petroleum ether) to afford methyl 3-(3-(4-(4-(trifluoromethyl)phenyl)-1*H*-indol-1-yl)benzylamino)benzoate (42 mg, 97% yield) as a pale purple viscous oil; ^{1}H NMR (400 MHz, $CDCl_3$): δ 7.81 (d, J = 8.20 Hz, 2H), 7.74 (d, J = 7.68 Hz, 2H), 7.55–7.32 (m, 8H), 7.28–7.20 (m, 3H), 6.82 (dd, J = 5.12, 2.15 Hz, 1H), 6.79 (d, J = 3.26 Hz, 1H), 4.50 (s, 2H), 3.88 (s, 3H). Calcd mass for $C_{30}H_{23}F_3N_2O_2$: 500.51; LRMS (ESI) m/z $[M+H]^+$ = 501.35. To a solution of methyl 3-(3-(4-(4-(trifluoromethyl)phenyl)-1*H*-indol-1-yl)benzylamino)-

benzoate (40 mg, 0.080 mmol) in THF/MeOH/H_2O (1:1:1) was added 1.0 M aqueous solution of LiOH/H_2O (33.5 mg, 0.80 mmol) and the reaction mixture was allowed to stirred at room temperature until the completion of reaction as judged by TLC. After evaporation of THF, the solution was acidified with 1 N HCl and extracted with ethyl acetate (3 × 25 mL), the organic layer was washed with water (20 mL), dried over Na_2SO_4, concentrated under reduced pressure and purified by chromatography (5 g silica gel, 0–5% methanol–dichloromethane) to afford compound **19**, (33 mg, 0.068 mmol, 85 % yield) as white powder. ^{1}H NMR (400 MHz, $CDCl_3$+CD_3OD): δ 7.81 (d, J = 7.39 Hz, 2H), 7.74 (d, J = 7.95 Hz, 2H), 7.54 (s, 1H), 7.50 (dd, J = 13.64, 7.74 Hz, 2H), 7.45 (d, J = 9.28 Hz, 2H), 7.41–7.38 (m, 3H), 7.26–7.21 (m, 3H), 6.84 (dd, J = 7.75, 1.16 Hz, 1H), 6.79 (d, J = 3.05 Hz, 1H), 4.50 (s, 2H). Calcd mass for $C_{29}H_{21}F_3N_2O_2$: 486.16; LRMS (ESI) m/z $[M+H]^+$ = 487.40.

4.3. General inhibition studies in ELISA

Streptavidin-coated plates (PerkinElmer Life Sciences) were washed one time with reaction buffer (50 mM Tris, 1 mM EDTA, 1 mg/mL BSA, 4% DMSO, 0.5 mM DTT, 0.1% Triton-X, pH 8.0). SET7 at 2.8 nM and SAM at 300 nM were diluted in reaction buffer and added in a volume of 16 μL. Control wells received only SET7. Test compounds (0.2 μL, 5 mM) were added and plates were incubated for 5 min at room temperature with gentle agitation. The reactions were initiated by the addition of 900 nM H3(1–20)-cys-biotin substrate in reaction buffer in a volume of 16 μL, and plates were incubated for an additional 5 min at 30 °C. Plates were aspirated, and the reaction was terminated by the addition of 100 μL of 50 mM sodium acetate, pH 5.0. After 5 min, plates were washed two times in 50 μL wash buffer (50 mM Tris, 150 mM NaCl, 0.05% Tween-20, 10 mg/mL BSA, pH 8.0) and incubated for one hour in 50 μL block buffer (50 mM Tris, 250 mM NaCl, 50 mg/mL BSA, pH 8.0) at room temperature. Plates were washed one time in wash buffer and incubated in 35 μL wash buffer containing 2 ng/μL rabbit-α-H3-monomethyl-K4 (Millipore) at room temperature for 1.5 h. Plates were then washed three times in 50 μL wash buffer, followed by addition of 35 μL wash buffer containing 0.1 ng/μL donkey-α-rabbit-HRP (Jackson ImmunoResearch). After 30 min incubation at room temperature, plates were washed one time in 50 μL wash buffer and two times in (TBS 20 mM Tris, 150 mM NaCl, pH 8.0), and 50 μL LumiGLO substrate (KPL) was added. Luminescence was measured on an EnVision 2101 Plate Reader (PerkinElmer Life Sciences) with a 0.1 s acquisition time. Activity values were determined by dividing luminescence counts for each compound concentration by luminescence of internal DMSO control for that compound. Dose–response curve were constructed and IC_{50} values were calculated using parameter logistic equation by KaleidagGraph software.

4.4. General inhibition studies in SPA: scintillation proximity assay (SPA) protocol

For each sample, 12 μL of reaction buffer (50 mM Tris, pH 8.5, 1 mg/mL BSA, 1 mM EDTA, 1 mM DTT) containing SET7 (25 nM), H3(1–20)-cys-biotin (900 nM), and test compound in DMSO (2% final) were incubated at 30 °C for 5 min. Methyltransferase reactions were initiated by addition of unlabeled 3 μL *S*-adenosyl methionine (SAM; 2 μM) containing a trace amount of ^{3}H-SAM (0.2 μM), and samples were incubated at 30 °C. After 8 min, 10 μL was removed from each sample and added to 100 μL Streptavidin-coated SPA beads (Perkin Elmer; 0.9375 mg/mL) in quench buffer (50 mM sodium acetate, pH 5.0, 1 mg/mL BSA, 1 mM EDTA, 10% glycerol, 1 mM unlabeled SAM) in white clear-bottomed 384 plates (BD Falcon). Counts per minute (CPM) for each sample were measured using a Microbeta Trilux counter (Perkin Elmer). Testing was performed twice ($n \geqslant 2$). Background was subtracted and percent activity was determined by dividing CPM for each sample by CPM of the negative (DMSO only) control and multiplying by 100.

Acknowledgments

TMK is grateful to the NIH (GM98579) and the Leukemia and Lymphoma Society for support.

Supplementary data

Supplementary data (dose–response curve of compound **19** against the Set7 in ELISA (Fig. S1); general experimental procedures and characterization data for compounds **20**–**35**) associated with this article can be found, in the online version, at http://dx.doi.org/10.1016/j.bmc.2014.02.024. These data include MOL files and InChiKeys of the most important compounds described in this article.

References and notes

1. Strahl, B. D.; Allis, C. D. *Nature* **2000**, *403*, 41.
2. Jenuwein, T.; Allis, C. D. *Science* **2001**, *293*, 1074.
3. Biel, M.; Wascholowski, V.; Giannis, A. *Angew. Chem., Int. Ed.* **2005**, *44*, 3186.
4. Luger, K.; Mader, A. W.; Richmond, R. K.; Sargent, D. F.; Richmond, T. J. *Nature* **1997**, *389*, 251.
5. Gelato, K. A.; Fischle, W. *Biol. Chem.* **2008**, *389*, 353.
6. Martin, C.; Zhang, Y. Nature Rev *Mol. Cell. Biol.* **2005**, *6*, 838.
7. Grunstein, M. *Nature* **1997**, *389*, 349.
8. Lachner, M.; Jenuwein, T. *Curr. Opin. Cell Biol.* **2002**, *14*, 286.
9. Ruthenburg, A. J.; Allis, C. D.; Wysocka, J. *J. Mol. Cell* **2007**, *25*, 15.
10. Sims, R. J.; Reinberg, D. *Genes Dev.* **2006**, *20*, 2779.
11. Mosammaparast, N.; Shi, Y. *Annu. Rev. Biochem.* **2010**, *179*, 155.
12. Duncan, E. M.; Allis, C. D. *Prog. Drug Res.* **2011**, *67*, 69.
13. Kouzarides, T. *Cell* **2007**, *128*, 693.
14. Copeland, R. A.; Solomon, M. E.; Richon, V. M. *Nat. Rev. Drug Disc.* **2009**, *8*, 724.
15. Kubicek, S.; O'Sullivan, R. J.; August, E. M.; Hickey, E. R.; Zhang, Q.; Teodoro, M. L.; Rea, S.; Mechtler, K.; Kowalski, J. A.; Homon, C. A.; Kelly, T. A.; Jenuwein, T. *Mol. Cell* **2007**, *25*, 473.
16. Yao, Y.; Chen, P.; Diao, J.; Cheng, G.; Deng, L.; Anglin, J. L.; Prasad, B. V. V.; Song, Y. *J. Am. Chem. Soc.* **2011**, *133*, 16746.
17. Mori, S.; Iwase, K.; Iwanami, N.; Tanaka, Y.; Kagechika, H.; Hirano, T. *Bioorg. Med. Chem.* **2010**, *18*, 8158.
18. Noble, M. E. M.; Endicott, J. A.; Johnson, L. N. *Science* **2004**, *303*, 1800.
19. Trievel, R. C.; Beach, B. M.; Dirk, L. M. A.; Houtz, R. L.; Hurley, J. H. *Cell* **2002**, *111*, 91.
20. Xiao, B.; Jing, C.; Wilson, J. R.; Walker, P. A.; Vasisht, N.; Kelly, G.; Howell, S.; Taylor, I. A.; Blackburn, G. M.; Gamblin, S. J. *Nature* **2003**, *421*, 652.
21. Huang, S. *Nat. Rev. Cancer* **2002**, *2*, 469.
22. Dirk, L. M. A.; Flynn, E. M.; Dietzel, K.; Couture, J.-F.; Trievel, R. C.; Houtz, R. L. *Biochemistry* **2006**, *46*, 3905.
23. Barbés, C.; Sánchez, J.; Yebra, M. J.; Robert-Geró, M.; Hardisson, C. *FEMS Microbiol. Lett.* **1990**, *57*, 239.
24. Yebra, M. J.; Sanchez, J.; Martin, C. G.; Hardisson, C.; Barbés, C. *J. Antibiot. (Tokyo)* **1991**, *44*, 1141.
25. Kumar, R.; Srivastava, R.; Singh, R. K.; Surolia, A.; Rao, D. N. *Bioorg. Med. Chem.* **2008**, *16*, 2276.
26. Peters, U.; Cherian, J.; Kim, H. J.; Kwok, B. H.; Kapoor, T. M. *Nat. Chem. Biol.* **2006**, *2*, 618.
27. Islam, K.; Chin, H. F.; Olivares, A. O.; Saunders, L. P.; De-la-cruz, E. M.; Kapoor, T. M. *Angew. Chem., Int. Ed.* **2010**, *49*, 8484.
28. See Supporting information.
29. Wilson, J. R.; Jing, C.; Walker, P. A.; Martin, S. R.; Howell, S. A.; Blackburn, G. M.; Gamblin, S. J.; Xiao, B. *Cell* **2002**, *111*, 105.
30. Wu, J.; Cheung, T.; Grande, C.; Ferguson, A. D.; Zhu, X.; Theriault, K.; Code, E.; Birr, C.; Keen, N.; Chen, H. *Biochemistry* **2011**, *50*, 6488.
31. Collins, R. E.; Tachibana, M.; Tamaru, H.; Smith, K. M.; Jia, D.; Zhang, X.; Selker, E. U.; Shinkai, Y.; Cheng, X. *J. Biol. Chem.* **2005**, *280*, 5563.
32. Habig, M.; Blechschmidt, A.; Dressler, S.; Hess, B.; Patel, V.; Billich, A.; Ostermeier, C.; Beer, D.; Klumpp, M. *J. Biomol. Screening* **2009**, *14*, 679.